

Global Scaling of Planetary Systems

Hartmut Müller

E-mail: hm@interscalar.com

The paper introduces a scale-invariant model of matter as fractal chain system of oscillating protons and electrons that is applied to the analysis of the solar system and extra-solar planetary systems. Based on global scaling, an explanation of the large number of coincident metric characteristics in different planetary and moon systems is proposed.

Introduction

The formation and evolution of the solar system is caused by very different processes and it is a complex field of research that considers electromagnetic, thermodynamic, hydrodynamic, nuclear physical and chemical factors in their complex interaction. Advanced models were developed [1–5] in the last century which explain essential features of the solar system formation. Gravity is treated as dominant force at macroscopic scales that forms the shape and trajectory (orbit) of astronomical bodies including stars and galaxies. Indeed, if numerous bodies are gravitationally bound to one another, classic models predict long-term highly unstable states that contradict with the astrophysical reality in the solar system.

Furthermore, many metric characteristics of the solar system are not predicted in standard models. A remarkably large number of coincidences are considered to be casual and are not even topics of theoretical research. For example, Mars and Mercury, but also Uranus and Venus have the same surface gravity acceleration. Such dissimilar bodies like Jupiter and Ceres, but also Earth, Mars and Eris have similar rotation periods. Various moons of very different planets in the solar system have the same orbital periods as have various planets in different extrasolar systems like Trappist 1 or Kepler 20.

In this paper we apply our scale-invariant model [6–8] of matter as fractal chain system of oscillating protons and electrons to the analysis of the solar system and extrasolar planetary systems. Based on our hypothesis of global scaling we propose an explanation of the large number of coincidences of the metric characteristics of the systems.

Methods

As result of measurement, real numbers build the bridge that connects theoretical models with the physical reality [9]. The classification of real numbers, in particular the difference between rational and irrational numbers is not only a mathematical task. It is also an essential aspect of stability in real systems. Parameter relations corresponding to rational numbers of small quotients support resonance interactions inside the system and make the system unstable. On the contrary, irrational relations correspond to minimum resonance interaction inside the system and to its stability [10].

Indeed, this stability can be lasting only if a given irrational relation cannot be transformed into a rational by elementary arithmetic operations.

In the case of algebraic numbers, an irrational relation of wavelengths can lead to rational relations of surfaces, volumes, masses or energies and nevertheless can make the system unstable.

Transcendental numbers cannot be represented as roots of algebraic equations. Therefore, no elementary arithmetic operation like addition or multiplication can transform a transcendental number into a rational. This is not valid for irrational, but non transcendental numbers, including the so-called golden number $\phi = (\sqrt{5}+1)/2$.

It is remarkable that only continued fractions deliver bi-unique representations of all real numbers, rational and irrational. Finite continued fractions represent always rational numbers, whereas infinite continued fractions represent irrational numbers. That is why any irrational number can be approximated by finite continued fractions - the convergents which deliver always the best and quickest approximation [11]. It is notable that the best rational approximation of an irrational number by a finite continued fraction is not a task of computation, but only an act of termination of the fractal recursion.

Alas, transcendental numbers can be approximated exceptionally well by rational numbers, because their continued fractions contain large denominators and can be truncated with minimum loss of precision. For instance, the fourth denominator in the simple continued fraction of $\pi = [3; 7, 15, 1, 292, \dots] = 3.1415927\dots$ is quite big, so that the ratio $355/113 \approx 3.1415929$ delivers a very good approximation. Euler's number $e = 2.71828\dots$ is also transcendental and can be represented as continued fraction with quickly increasing denominators, so that already the ratio $193/71 \approx 2.71831$ gives a good approximation.

In the consequence, transcendental numbers define the preferred relations of parameters which sustain the stability of a complex system. In this way, the system avoids destabilizing resonance. At the same time, a good rational approximation can be induced quickly, if resonance interaction is required. Furthermore, if stability is provided concerning all derivatives of a process, Euler's number is the only choice, because of the self-similarity of the natural exponential function regarding its derivatives:

$$\frac{d}{dx} e^x = e^x.$$

PROPERTY	ELECTRON	PROTON
rest mass m	$9.10938356(11) \cdot 10^{-31}$ kg	$1.672621898(21) \cdot 10^{-27}$ kg
energy $E = mc^2$	0.5109989461(31) MeV	938.2720813(58) MeV
angular frequency $\omega = E/\hbar$	$7.76344071 \cdot 10^{20}$ Hz	$1.42548624 \cdot 10^{24}$ Hz
angular oscillation period $\tau = 1/\omega$	$1.28808867 \cdot 10^{-21}$ s	$7.01515 \cdot 10^{-25}$ s
angular wavelength $\lambda = c/\omega$	$3.8615926764(18) \cdot 10^{-13}$ m	$2.1030891 \cdot 10^{-16}$ m
angular acceleration $a = c/\omega$	$2.327421 \cdot 10^{29}$ ms ⁻²	$4.2735 \cdot 10^{32}$ ms ⁻²

Table 1: The basic set of physical properties of the electron and proton. (c is the speed of light in a vacuum, \hbar is the reduced Planck constant, k_B is the Boltzmann constant). Data taken from Particle Data Group [20]. Frequencies, oscillation periods, accelerations and the proton wavelength are calculated.

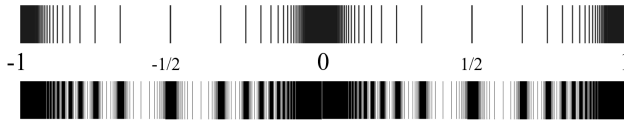


Fig. 1: The distribution of eigenvalues of \mathcal{F} for $k=1$ (above) and for $k=2$ (below) in the range $-1 \leq \mathcal{F} \leq 1$.

In [12] we have shown that the set of natural frequencies (eigenstates) of a fractal chain system of harmonic oscillators can be described as set (1) of finite continued fractions \mathcal{F} , which are natural logarithms:

$$\mathcal{F} = \ln(\omega_{jk}/\omega_{00}) = [n_{j0}; n_{j1}, n_{j2}, \dots, n_{jk}] \quad (1)$$

where ω_{jk} is the set of angular frequencies and ω_{00} is the fundamental frequency of the set. The denominators are integer: $n_{j0}, n_{j1}, n_{j2}, \dots, n_{jk} \in \mathbb{Z}$, the cardinality $j \in \mathbb{N}$ of the set and the number $k \in \mathbb{N}$ of layers are finite. In the canonical form, all numerators equal 1.

Any finite continued fraction represents a rational number. Therefore, all frequency ratios ω_{jk}/ω_{00} in (1) are irrational, because for rational exponents the natural exponential function is transcendental [13]. This circumstance provides for high stability of the eigenstates (1) of a chain system of harmonic oscillators because it prevents resonance interaction between the elements of the system. In [14–16] we have applied continued fractions of the type (1) as criterion of stability in engineering.

In the canonical form, the distribution density of eigenvalues of finite continued fractions reaches maxima near reciprocal integers $1, 1/2, 1/3, 1/4, \dots$ which are the attractor points in the fractal set \mathcal{F} of natural logarithms (fig. 1).

Shorter continued fractions (1) with smaller denominators correspond with more stable eigenstates of the chain system, because the logarithmic distance between their eigenvalues is maximum. Considering the existence of two complementary fractals on the sets of rational and irrational numbers accordingly [17], the probability that small variations (fluctuations)

lead to coincidences between irrational and rational numbers of small quotients is minimum. Therefore, integer and half logarithms represent the most stable eigenstates.

Already in 1950 Gantmacher and Krein [18] have demonstrated that continued fractions are solutions of the Euler-Lagrange equation for low amplitude harmonic oscillations in simple chain systems. Terskich [19] generalized this method for the analysis of oscillations in branched chain systems. In [6] the continued fraction method was extended to the analysis of chain systems of harmonic quantum oscillators.

In the case of harmonic quantum oscillators, the continued fractions (1) define not only fractal sets of natural angular frequencies ω_{jk} , angular accelerations $a_{jk} = c \cdot \omega_{jk}$, oscillation periods $\tau_{jk} = 1/\omega_{jk}$ and wavelengths $\lambda_{jk} = c/\omega_{jk}$ of the chain system, but also fractal sets of energies $E_{jk} = \hbar \cdot \omega_{jk}$ and masses $m_{jk} = E_{jk}/c^2$ which correspond with the eigenstates of the system [8].

In this way, the continued fractions (1) generate the fundamental fractal \mathcal{F} of eigenstates in chain systems of harmonic quantum oscillators.

As the cardinality and number of layers of the continued fractions (1) are finite but not limited, in each point of the space-time occupied by the chain system of harmonic quantum oscillators the scalar \mathcal{F} is defined. Therefore, any chain system of harmonic quantum oscillators can be seen as source of the fractal scalar field \mathcal{F} , the fundamental field of the system. The scalar potential difference $\Delta\mathcal{F}$ of sequent equipotential surfaces at a given layer k is defined by the difference of continued fractions (1). In the canonical form:

$$\begin{aligned} \Delta\mathcal{F} &= \mathcal{F}(j,k) - \mathcal{F}(j+1,k) = \\ &= [n_{j0}; n_{j1}, n_{j2}, \dots, n_{jk}] - [n_{j0}; n_{j1}, n_{j2}, \dots, n_{j+1,k}]. \end{aligned}$$

In [7] we have introduced a scale-invariant model of matter as fractal chain system of harmonically oscillating protons and electrons that generates the fundamental field \mathcal{F} . Normal matter is formed by nucleons and electrons because they are exceptionally stable quantum oscillators. In the concept of isospin, proton and neutron are viewed as two states of the

same quantum oscillator. Furthermore, they have similar rest masses. However, a free neutron decays into a proton, an electron and antineutrino within 15 minutes while the life-spans of the proton and electron top everything that is measurable, exceeding 10^{29} years [20].

The exceptional stability of electron and proton predestinate their physical characteristics as fundamental units. Table 1 shows the basic set of electron and proton units that can be considered as a fundamental metrology. In [8] was shown that it is compatible with Planck units [21].

Within our model, the proton-to-electron ratio (tab. 1) is caused by the fundamental field \mathcal{F} . In fact, the natural logarithm is close to rational:

$$\ln \frac{938.2720813 \text{ MeV}}{0.5109989461 \text{ MeV}} \approx 7 + \frac{1}{2}.$$

As a consequence, the fundamental field of the proton is complementary to that of the electron, because integer logarithms of the proton \mathcal{F} correspond to half logarithms of the electron \mathcal{F} and vice versa, so that the scaling factor \sqrt{e} connects similar equipotential surfaces of the proton field with those of the electron field in alternating sequence [8].

We hypothesize that scale invariance of the fundamental field \mathcal{F} calibrated on the physical properties of the proton and electron (tab. 1) is a universal characteristic of organized matter and criterion of stability. This hypothesis we have called Global Scaling [22].

Results

Within our scale-invariant model of matter [7], atoms and molecules emerge as eigenstates of stability in fractal chain systems of harmonically oscillating protons and electrons.

Andreas Ries [23] demonstrated that this model allows for the prediction of the most abundant isotope of a given chemical element. From this point of view, any physical body, being solid, liquid or gas can be seen as fractal chain system of oscillating molecules, atoms, ions, protons and electrons that follows the fundamental field \mathcal{F} .

Therefore, in the framework of our fractal model of matter, the fundamental field \mathcal{F} affects any type of physical interaction, regardless of its complexity.

In [24] we applied our model to the analysis of gravimetric and seismic characteristics of the Earth and could show that our estimations [25] correspond well with established empiric models of the Earth interior.

In [26] we did demonstrate that the vertical sequence of stable atmospheric layers corresponds with the sequence of main spatial equipotential surfaces of the fundamental field \mathcal{F} , not only at Earth, but also at Venus, Mars and Titan.

In [27] was demonstrated that the mass distribution in the solar system and the mass distribution of elementary particles follow the same scaling law. In [8] was shown that the distribution of rotation and orbital periods in the solar system

corresponds with main temporal equipotential surfaces of the fundamental field \mathcal{F} .

For verification of Global Scaling in this paper we consider only direct measurements and refer on data that should not contain systematic errors. As such data we consider the rotation and orbital periods, but also the majority of estimated body radii and orbital distances in the solar system.

Fig. 2 shows the correspondence of orbital periods for planets and planetoids of the solar system with equipotential surfaces of the fundamental field \mathcal{F} . Tab. 2 contains the corresponding data. Integer numbers in the bottom of the graphic are natural logarithms of main equipotential surfaces $[n_0; \infty]$ of the fundamental field \mathcal{F} calibrated on the proton (bold) and electron (thin). For example, Jupiter's orbital period [28] corresponds with the main temporal equipotential surface $[66; \infty]$ of the fundamental field \mathcal{F} calibrated on the oscillation period of the electron:

$$\ln \left(\frac{T_{\text{Jupiter}}}{\tau_{\text{electron}}} \right) = \ln \left(\frac{4332.59 \cdot 86400 \text{ s}}{2\pi \cdot 1.28808867 \cdot 10^{-21} \text{ s}} \right) = 66.00$$

The logarithmic scale in fig. 2 covers a range of 79 to 235000 days \approx 640 years.

Fig. 3 shows the correspondence of orbital periods for moons of the solar system and planets of the systems Trappist 1 [29] and Kepler 20 [30] with temporal equipotential surfaces of the fundamental field \mathcal{F} . Tab. 3 and 4 contain the corresponding data. It is remarkable that the orbits of Trappist 1b, c, d and e correspond with main equipotential surfaces of the fundamental field \mathcal{F} . This is also valid for Kepler 20b, c, d and e and for many other exoplanetary systems we did not include in this paper.

Because of the complementarity of the fundamental field of the proton to that of the electron, equipotential surfaces of the type $[n_{j0}; \pm 2]$ coincide always with complementary

body	orbital period T, d	$\ln (T/2\pi \tau_e)$	\mathcal{F}
Eris (P)	203830	69.86	[70; -6]
Pluto (P)	90560	69.04	[69; ∞]
Neptune	60182	68.64	[69; -3]
Uranus	30688.5	67.96	[68; ∞]
Saturn	10759.22	66.91	[67; ∞]
Jupiter	4332.59	66.00	[66; ∞]
Ceres (P)	1681.63	65.06	[65; ∞]
Mars	686.971	64.16	[64; 6]
Earth	365.256363	63.53	[63; 2]
Venus	224.701	63.04	[65; ∞]
Mercury	87.9691	62.12	[62; 6]

Table 2: Natural logarithms of the orbital period-to-electron oscillation period ratios for planets and heaviest planetoids (P) of the solar system and the corresponding equipotential surfaces of the fundamental field \mathcal{F} . Data: [28]

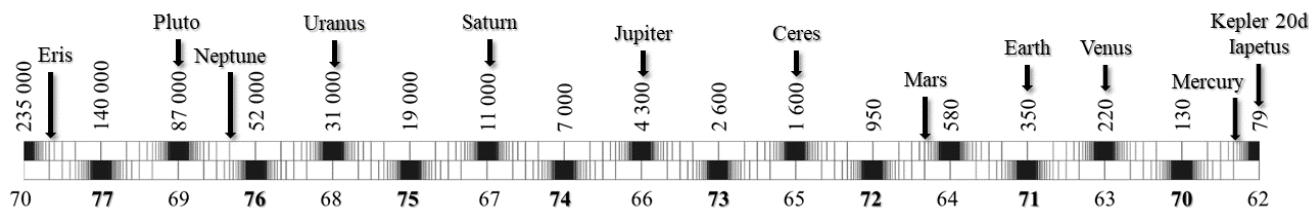


Fig. 2: Correspondence of orbital periods of planets and planetoids of the solar system with temporal equipotential surfaces of the fundamental field \mathcal{F} . Integers in the bottom of the graphic are natural logarithms of main equipotential surfaces $[n_{j0}; \infty]$ of the fundamental field \mathcal{F} calibrated on the proton (bold) and electron (thin). The logarithmic scale covers a range of 79 to 235 000 days \approx 640 years. Tab. 2 contains the corresponding data.

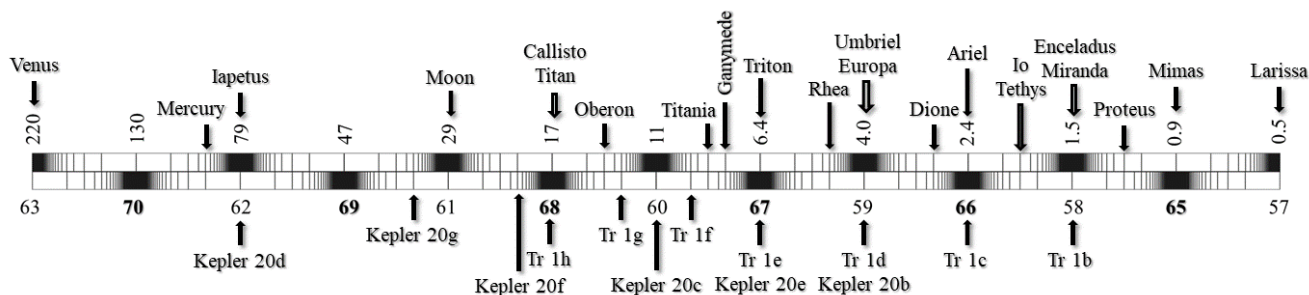


Fig. 3: Correspondence of orbital periods of moons of the solar system and planets of the systems Trappist 1 and Kepler 20 with temporal equipotential surfaces of the fundamental field \mathcal{F} . The logarithmic scale covers a range of 0.5 to 220 days. Tab. 3 and 4 contain the corresponding data.

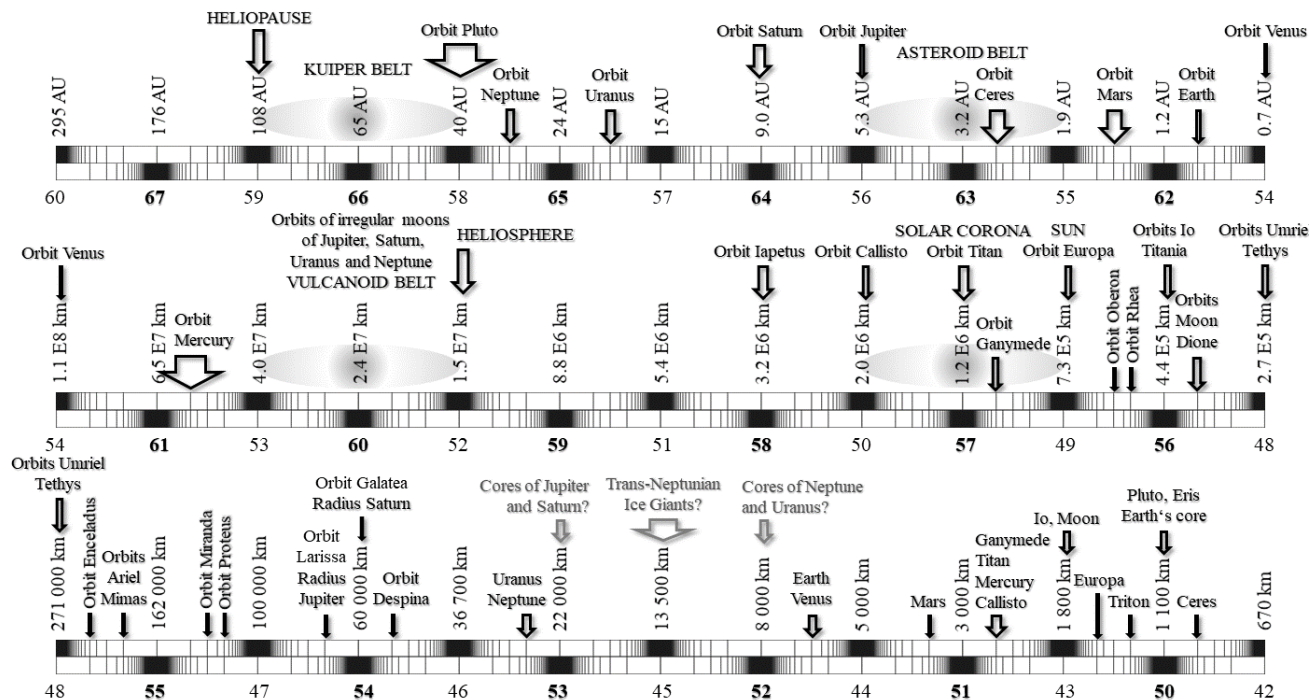


Fig. 4: Correspondence of metric characteristics of large structures in the solar system with spatial equipotential surfaces of the fundamental field \mathcal{F} . The logarithmic scale covers a range of 670 km to 295 AU. The width of the arrows is a measure of data dispersion or eccentricity of an orbit. Grey arrows and descriptions are hypothetical. The corresponding data are published in [8, 25].

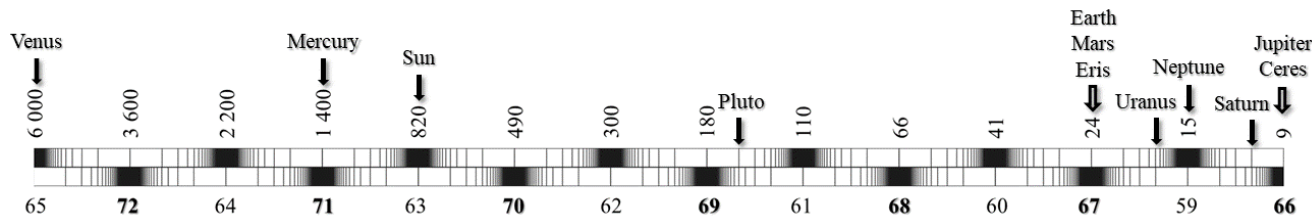


Fig. 5: Correspondence of rotation periods of planets and some planetoids of the solar system with temporal equipotential surfaces of the fundamental field \mathcal{F} . The logarithmic scale covers a range of 9 to 6000 hours. Tab. 5 contains the corresponding data.

main equipotential surfaces $[n_{j0}; \infty]$, so that the remaining orbits correspond mostly with equipotential surfaces of the type $[n_{j0}; \pm 3]$. This distribution is a consequence of the fractal hierarchy $1/2, 1/3, 1/4, \dots$ of stability layers (see fig. 1) given by the continued fraction (1) of natural logarithms.

Fig. 4 shows the correspondence of metric characteristics

moon of	orbital period T, d	$\ln(T/2\pi\tau_e)$	\mathcal{F}
EARTH			
Moon	27.321661	60.94	$[61; \infty]$
JUPITER			
Callisto	16.689	60.45	$[60; 2]$
Ganymede	7.1546	59.61	$[60; -3]$
Europa	3.5512	58.91	$[60; \infty]$
Io	1.7691	58.21	$[58; 4]$
SATURN			
Iapetus	79.3215	62.00	$[62; \infty]$
Titan	15.945	60.41	$[60; 2]$
Rhea	4.5182	59.14	$[59; 6]$
Dione	2.7369	58.65	$[59; -3]$
Tethys	1.8878	58.26	$[58; 4]$
Enceladus	1.3702	57.95	$[58; \infty]$
Mimas	0.942	57.57	$[57; 2]$
URANUS			
Oberon	13.4632	60.24	$[60; 4]$
Titania	8.7062	59.78	$[60; -4]$
Umbriel	4.144	59.05	$[59; \infty]$
Ariel	2.52	58.54	$[58; 2]$
Miranda	1.4135	57.98	$[58; \infty]$
NEPTUNE			
Nereid	360.1362	63.52	$[63; 2]$
Triton	5.877	59.41	$[59; 2]$
Proteus	1.1223	57.75	$[58; -4]$
Larissa	0.555	57.04	$[57; \infty]$

Table 3: Natural logarithms of the orbital period-to-electron oscillation period ratios for the largest moons of in the solar system and the corresponding equipotential surfaces of the fundamental field \mathcal{F} . Data: [31]

of large structures in the solar system with spatial equipotential surfaces of the fundamental field \mathcal{F} . The corresponding data are published in [8, 25]. For example, the visible equatorial radius of Saturn [32] corresponds with the main spatial equipotential surface $[54; \infty]$ of the fundamental field \mathcal{F} calibrated on the wavelength of the proton (tab. 1):

$$\ln\left(\frac{r_{\text{Saturn}}}{\lambda_{\text{proton}}}\right) = \ln\left(\frac{6.0268 \cdot 10^7 \text{ m}}{2.1030891 \cdot 10^{-16} \text{ m}}\right) = 54.01$$

The logarithmic scale in fig. 4 covers a range of 670 km to 295 AU. In general, the width of the arrows is a measure of data dispersion or eccentricity of an orbit. Grey arrows and descriptions are hypothetical.

Fig. 4 shows that the orbits of Venus, Jupiter, Saturn and Pluto correspond with main equipotential surfaces $[n_{j0}; \infty]$ of the fundamental field \mathcal{F} .

It is notable that Jupiter’s orbit represents the logarithmic mean between the orbits of Venus and Pluto. The orbits of

planet of	orbital period T, d	$\ln(T/2\pi\tau_e)$	\mathcal{F}
TRAPPIST 1			
H	18.767953	60.56	$[60; 2]$
G	12.354473	60.15	$[60; 6]$
F	9.205585	59.86	$[60; \infty]$
E	6.099615	59.45	$[59; 2]$
D	4.04961	59.03	$[59; \infty]$
C	2.4218233	58.51	$[58; 2]$
B	1.51087081	58.04	$[58; \infty]$
KEPLER 20			
D	77.61130017	61.98	$[62; \infty]$
G	34.94	61.17	$[61; 6]$
F	19.57758478	60.61	$[61; -3]$
C	10.85409089	60.01	$[60; \infty]$
E	6.09852281	59.45	$[59; 2]$
B	3.69611525	58.94	$[59; \infty]$

Table 4: Natural logarithms of the orbital period-to-electron oscillation period ratios for exoplanets of the systems Trappist 1 and Kepler 20 with the corresponding equipotential surfaces of the fundamental field \mathcal{F} . Data: [29, 30]

body	rotation period τ , h	$\ln(\tau/\tau_p)$	\mathcal{F}
Venus	5816.66728	72.48	[72; 2]
Mercury	1407.5	71.05	[71; ∞]
Sun	823.346	70.51	[70; 2]
Pluto (P)	152.87496	68.83	[69; -6]
Eris (P)	25.9	67.06	[67; ∞]
Mars	24.62278	67.01	[67; ∞]
Earth	23.93444	66.98	[67; ∞]
Uranus	17.24	66.66	[67; -3]
Neptune	16.11	66.57	[66; 2]
Saturn	10.55	66.16	[66; 6]
Jupiter	9.925	66.09	[66; ∞]
Ceres (P)	9.07417	66.01	[66; ∞]

Table 5: Natural logarithms of the rotation period-to-proton oscillation period ratios for planets and heaviest planetoids (P) of the solar system and the corresponding equipotential surfaces of the fundamental field \mathcal{F} . Data: [28].

Mercury, Earth, Mars, Ceres correspond all with equipotential surfaces of the type $[n_{j0}; \pm 3]$. This is valid also for the orbits of Ganymede, Rhea, Dione and the Moon. The orbits of Uranus and Neptune correspond with equipotential surfaces $[n_{j0}; \pm 4]$.

The orbits of Callisto, Europa, Io and Titan correspond with main equipotential surfaces $[n_{j0}; \infty]$. This is also valid for the orbits of Tethys, Umbriel, Titania and Iapetus.

The radius of the photosphere of the Sun and the visible radius of Saturn correspond with main spatial equipotential surfaces $[n_{j0}; \infty]$.

The visible radii of Jupiter, Uranus and Neptune, but also the radii of the solid bodies Mars, Mercury, Ganymede, Titan, Callisto, Europa and Ceres correspond all with equipotential surfaces of the type $[n_{j0}; \pm 3]$. Only the radii of Earth and Venus correspond with equipotential surfaces $[n_{j0}; \pm 4]$. The radii of Io, the Moon, Pluto and Eris correspond with main equipotential surfaces $[n_{j0}; \infty]$.

It is remarkable that the orbit of Europa coincides with the radius of the Sun (boundary of the photosphere), the orbit of Galatea (Neptune VI) coincides with Saturn's radius (stratopause) and the orbit of Larissa (Neptune VII) with the radius of Jupiter.

Fig. 5 shows the correspondence of rotation periods of planets and large planetoids of the solar system with temporal equipotential surfaces of the fundamental field \mathcal{F} . The logarithmic scale in fig. 5 covers a range of 9 to 6000 hours. Tab. 5 contains the corresponding data.

The rotation periods of Venus, Mercury, the Sun, Earth, Mars, Eris, Neptune, Jupiter and Ceres coincide with main equipotential surfaces while the rotation periods of Saturn, Uranus and Pluto correspond with temporal equipotential surfaces of the type $[n_{j0}; \pm 3]$.

Although the rotation of Venus [31] is retrograde, its rotation period of 5816.66728 hours fits perfectly with the main temporal equipotential surface [65; ∞] of the electron \mathcal{F} :

$$\ln\left(\frac{\tau_{\text{Venus}}}{\tau_{\text{electron}}}\right) = \ln\left(\frac{5816.66728 \cdot 3600 \text{ s}}{1.28808867 \cdot 10^{-21} \text{ s}}\right) = 64.96$$

Concluding our analysis of the solar system and exoplanetary systems we assume that planetary systems preferentially occupy main equipotential surfaces of the fundamental field \mathcal{F} . This circumstance makes possible the calculation of remaining orbits in exoplanetary systems.

Conclusion

The logarithmic projection of the fundamental field \mathcal{F} reveals the remarkable scale symmetry of the solar system and suggests that it could hardly be the consequence of random collisions. Within our cosmological hypothesis of Global Scaling [8], the formation of the solar system as well as exoplanetary systems can be understood in terms of harmonic oscillations in chain systems.

Movement along equipotential surfaces requires no work. That's why stable orbits correspond with equipotential surfaces of the fundamental field \mathcal{F} and orbital eccentricity is always limited by neighboring equipotential surfaces [8].

Equipotential surfaces of the fundamental field \mathcal{F} define not only stable planetary orbits, but also the metric characteristics of stratification layers in planetary atmospheres [26] and lithospheres [25]. From this point of view, metric characteristics of stable structures origin from the same fundamental field \mathcal{F} and differ only in scale.

The conceptual core of our model are harmonic oscillations in chain systems. These oscillations remain stable only if resonance interaction inside the system can be avoided. As solution survives a logarithmically fractal set (1) of transcendental frequency ratios. Note it is not a simple power law.

We suppose that basic power rules like the Titius-Bode [33], Dermott's rule [34] as well as the discovered golden number [35] and Fibonacci ratios [36] in solar planetary and satellite systems and in exoplanetary systems reflect a local feature of the fundamental field \mathcal{F} , because $\sqrt{e} = 1,648\dots$ is close to the golden number $\phi = 1.618\dots$ and for small exponents, the rounded up powers of the square root of Euler's number deliver the sequence of Fibonacci numbers.

Another essential aspect of our cosmological model [8] is Global Scaling, the hypothesis that in the universe there is only one global fundamental field \mathcal{F} . In fact, it was demonstrated that scale relations in particle physics [6, 7, 37] and nuclear physics [23, 38, 39], astrophysics [8, 27, 40–43], geophysics [25, 26] and biophysics [44, 45] follow always the same fundamental field \mathcal{F} calibrated on the proton and electron, without any additional or particular settings. The universality and unity of the fundamental field \mathcal{F} might signify that everything in the universe is part of one giant oscillating chain system.

Acknowledgements

The author is thankful to Oleg Kalinin, Alexej Petrukhin, Viktor Panchelyuga and Erwin Müller for valuable discussions and to Leili Khosravi for permanent support on all stages of the study.

Submitted on March 27, 2018

References

- Williams I. O., Cremin A.W. A survey of theories relating to the origin of the solar system. *Q. J. R. Astr. Soc.*, 1968, v. 9, 40–62.
- Alfvén H. Band Structure of the Solar System. Dermot S.F. Origin of the Solar System. pp. 41–48. Wiley, (1978).
- Woolfson M.M. The Solar System: Its Origin and Evolution. *Journal of the Royal Astronomical Society*, 1993, v. 34, 1–20.
- Van Flandern T. Our Original Solar System - a 21st Century Perspective. *MetaRes. Bull.* 17: 2–26, (2008). D21, 475–491, 2000.
- Woolfson M. M. Planet formation and the evolution of the Solar System. arXiv:1709.07294, (2017).
- Müller H. Fractal Scaling Models of Natural Oscillations in Chain Systems and the Mass Distribution of Particles. *Progress in Physics*, 2010, no. 3, 61–66.
- Müller H. Emergence of Particle Masses in Fractal Scaling Models of Matter. *Progress in Physics*, 2012, v. 4, 44–47.
- Müller H. Scale-Invariant Models of Natural Oscillations in Chain Systems and their Cosmological Significance. *Progress in Physics*, 2017, no. 4, 187–197.
- International Vocabulary of Metrology – Basic and General Concepts and Associated Terms. International Bureau of Weights and Measures, 2008, p. 16.
- Dombrowski K. Rational Numbers Distribution and Resonance. *Progress in Physics*, 2005, no. 1, 65–67.
- Khinchine A.Ya. Continued fractions. University of Chicago Press, Chicago, 1964.
- Müller H. Fractal Scaling Models of Resonant Oscillations in Chain Systems of Harmonic Oscillators. *Progress in Physics*, 2009, no. 2, 72–76.
- Hilbert D. Über die Transcendenz der Zahlen e und π . *Mathematische Annalen*, 1893, v. 43, 216–219.
- Müller H. The general theory of stability and objective evolutionary trends of technology. Applications of developmental and construction laws of technology in CAD. Volgograd, VPI, 1987 (in Russian).
- Müller H. Superstability as a developmental law of technology. Technology laws and their Applications. Volgograd-Sofia, 1989.
- Müller H., Otte R. Verfahren zur Stabilisierung von technischen Prozessen. PCT, WO 2005/071504 A2.
- Panchelyuga V. A., Panchelyuga M. S. Resonance and Fractals on the Real Numbers Set. *Progress in Physics*, 2012, no. 4, 48–53.
- Gantmacher F.R., Krein M.G. Oscillation matrixes, oscillation cores and low oscillations of mechanical systems. Leningrad, 1950.
- Terskich V.P. The continued fraction method. Leningrad, 1955.
- Olive K.A. et al. (Particle Data Group), *Chin. Phys. C*, 2016, v. 38, 090001. Patrignani C. et al. (Particle Data Group), *Chin. Phys. C*, 2016, v. 40, 100001.
- Planck M. Über Irreversible Strahlungsvorgänge. *Sitzungsberichte der Königlich Preussischen Akademie der Wissenschaften*, 1899, v. 1, 479–480.
- Müller H. Scaling as Fundamental Property of Natural Oscillations and the Fractal Structure of Space-Time. Foundations of Physics and Geometry. Peoples Friendship University of Russia, 2008 (in Russian).
- Ries A. Qualitative Prediction of Isotope Abundances with the Bipolar Model of Oscillations in a Chain System. *Progress in Physics*, 2015, v. 11, 183–186.
- Müller H. Gravity as Attractor Effect of Stability Nodes in Chain Systems of Harmonic Quantum Oscillators. *Progress in Physics*, 2018, v. 14, 19–23.
- Müller H. Quantum Gravity Aspects of Global Scaling and the Seismic Profile of the Earth. *Progress in Physics*, 2018, v. 14, 41–45.
- Müller H. Global Scaling of Planetary Atmospheres. *Progress in Physics*, 2018, v. 14, 66–70.
- Müller H. Fractal scaling models of natural oscillations in chain systems and the mass distribution of the celestial bodies in the Solar System. *Progress in Physics*, 2010, no. 4, 44–47.
- Jupiter Fact Sheet. nssdc.gsfc.nasa.gov
- Gillon M. et al. Seven temperate terrestrial planets around the nearby ultracool dwarf star TRAPPIST-1. *Nature*, 2017, 21360.
- Hand E. Kepler discovers first Earth-sized exoplanets. *Nature*, 2011, 9688.
- Venus Fact Sheet. nssdc.gsfc.nasa.gov
- Saturn Fact Sheet. nssdc.gsfc.nasa.gov
- Hayes W. Fitting random stable solar systems to Titius-Bode laws. arXiv: astro-ph/9710116v1 10 Oct 1997.
- Dermott S.F. On the origin of commensurabilities in the solar system - II: The orbital period relation. *Mon. Not. R. Astron. Soc.*, 1968, v. 141(3), 363–376.
- Butusov K. P. The Golden Ratio in the Solar System. Problems of Cosmological Research, v. 7, Moscow – Leningrad, 1978 (in Russian).
- Pletser V. Orbital Period Ratios and Fibonacci Numbers in Solar Planetary and Satellite Systems and in Exoplanetary Systems. arXiv:1803.02828 [physics.pop-ph], 2018.
- Ries A., Fook M. Fractal Structure of Nature's Preferred Masses: Application of the Model of Oscillations in a Chain System. *Progress in Physics*, 2010, no. 4, 82–89.
- Ries A. A Bipolar Model of Oscillations in a Chain System for Elementary Particle Masses. *Progress in Physics*, 2012, no. 4, 20–28.
- Ries A. The Radial Electron Density in the Hydrogen Atom and the Model of Oscillations in a Chain System. *Progress in Physics*, 2012, no. 3, 29–34.
- Müller H. Scaling of Body Masses and Orbital Periods in the Solar System. *Progress in Physics*, 2015, no. 2, 133–135.
- Müller H. Scaling of Moon Masses and Orbital Periods in the Systems of Saturn, Jupiter and Uranus. *Progress in Physics*, 2015, no. 2, 165–166.
- Müller H. Scaling of body masses and orbital periods in the Solar System as consequence of gravity interaction elasticity. Abstracts of the XII. International Conference on Gravitation, Astrophysics and Cosmology, dedicated to the centenary of Einstein's General Relativity theory. Moscow, PFUR, 2015.
- Müller H. Global Scaling as Heuristic Model for Search of Additional Planets in the Solar System. *Progress in Physics*, 2017, no. 4, 204–206.
- Müller H. Chain Systems of Harmonic Quantum Oscillators as a Fractal Model of Matter and Global Scaling in Biophysics. *Progress in Physics*, 2017, no. 4, 231–233.
- Müller H. Astrobiological Aspects of Global Scaling. *Progress in Physics*, 2018, v. 14, 3–6.